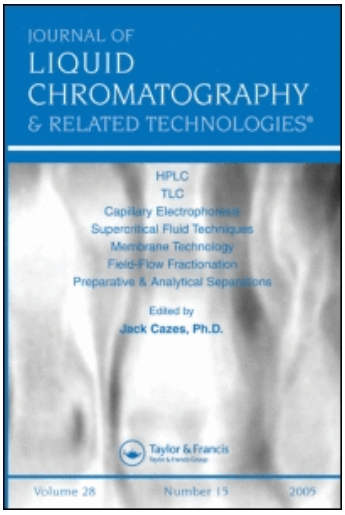

Journal of Liquid Chromatography & Related Technologies
Publication details, including instructions for authors and subscription information:
http://www.informaworld.com/smpp/title~content=t713597273

Three-Dimensional Isoviscous Flow Velocity Profiles and Resolution in Channels with Modulated Cross-Sectional Permeability for Focusing Field-Flow Fractionation

Josef Janča[a]
[a] Ecole Supérieure de Physique et Chimie Industrielles Laboratoire de Physique et Mécanique des Milieux Hétérogènes (URA CNRS 857), Paris Cedex 05, France

To cite this Article Janča, Josef(1991) 'Three-Dimensional Isoviscous Flow Velocity Profiles and Resolution in Channels with Modulated Cross-Sectional Permeability for Focusing Field-Flow Fractionation', Journal of Liquid Chromatography & Related Technologies, 14: 18, 3317 — 3330
To link to this Article: DOI: 10.1080/01483919108049393
URL: http://dx.doi.org/10.1080/01483919108049393

JOURNAL OF LIQUID CHROMATOGRAPHY, 14(18), 3317-3330 (1991)

THREE-DIMENSIONAL ISOVISCOUS FLOW VELOCITY PROFILES AND RESOLUTION IN CHANNELS WITH MODULATED CROSS-SECTIONAL PERMEABILITY FOR FOCUSING FIELD-FLOW FRACTIONATION

JOSEF JANČA
Ecole Supérieure de Physique et Chimie Industrielles
Laboratoire de Physique et Mécanique des Milieux Hétérogènes
(URA CNRS 857)
10 rue Vauquelin
75231 Paris Cedex 05, France

ABSTRACT

The form of the flow velocity profile developed in a carrier liquid flowing in separation channel for focusing field-flow fractionation can be controlled by manipulating the shape of the channel cross-section. The velocity profiles established in modulated cross-sectional permeability channels under the conditions of isoviscous flow were described previously by using the approximate solution of Navier-Stokes equation. In this paper, the previous approach is compared with an exact solution. The theoretical resolution is calculated for the actual trapezoidal cross-section channels and compared with the experimentally achieved resolutions. A fair agreement between the calculated and experimental resolutions was obtained.

INTRODUCTION

The shape of the flow velocity profile and the resolution in channels with modulated cross-sectional permeability were studied previously [1]. Takahashi and Gill's approximate equation [2], describing the flow velocity profile formed in

rectangular cross-section channel, was modified in order to describe the flow velocity profiles in trapezoidal and parabolic cross-section channels. The inaccuracy introduced by the approximation was estimated to be negligible. The use of the approximate description of the flow velocity profile is justified whenever the accurate analytical solution does not exist or the approximation facilitates the tractability of the resulting equations and providing the approximation does not neglect the important details of the shape of the flow velocity profile. A detailed analysis of the three-dimensional isoviscous flow velocity profile established in rectangular and trapezoidal cross-section channels is presented here. The resolution in focusing field-flow fractionation methods (focusing FFF) is discussed with respect to the operational conditions applied in real experiments and to the time of separation.

THEORETICAL ANALYSIS

Flow velocity profiles

The starting point of the analysis is the approximate equation for the flow velocity profile established in rectangular cross-section channel published by Takahashi and Gill [2]:

$$u_a(y,z) = \frac{k\, b^2\, \Delta P}{\mu\, L}\left(1 - \frac{y^2}{b^2}\right)\left(1 - \frac{\cosh(\sqrt{3}\, a\, \frac{z}{c})}{\cosh(\sqrt{3}\, a)}\right) \qquad (1)$$

where $u_a(y,z)$ is the local linear velocity of the flow in coordinates y,z, ΔP is the pressure drop along the channel of the length L, μ is the carrier liquid viscosity, k is a numerical constant corresponding to the given geometry of the channel (for instance k = 1/2 for rectangular cross-section channel), b and c are the half thickness and width resp. of the rectangular cross-section channel, and a = c/b is the aspect ratio. The system of coordinates demonstrated in Fig.1 is the same as in ref. [1], i.e., x-axis coincides with the longitudinal centerline of the channel and corresponds to the direction of the flow, y and z axes lie in the plane of the cross section of the channel, the origin is situated at the beginning of the channel.

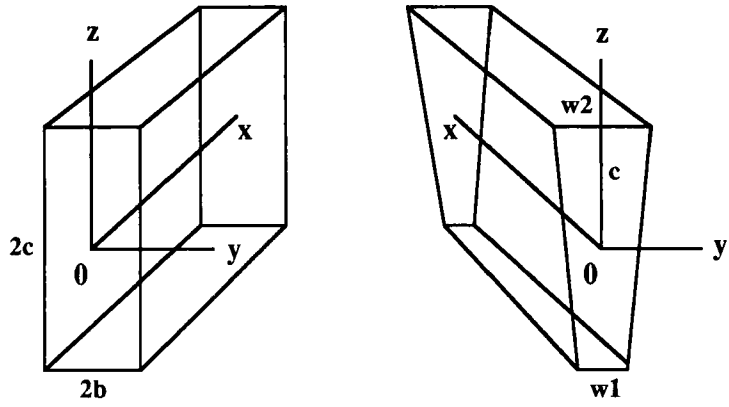

Fig.1. System of coordinates for rectangular and trapezoidal cross-section channels.

In the normalized coordinates, defined as Y = y/b and Z = z/c, Eq.(1) can be rewritten as:

$$u_a(Y,Z) = \frac{k\, b^2\, \Delta P}{\mu\, L} \left(1 - Y^2 \right) \left(1 - \frac{\cosh(\sqrt{3}\, a\, Z)}{\cosh(\sqrt{3}\, a)} \right) \qquad (2)$$

For the centerline velocity at coordinates Y = 0 and Z = 0 it holds:

$$u_a(0,0) = \frac{k\, b^2\, \Delta P}{\mu\, L} \left(1 - \frac{1}{\cosh(\sqrt{3}\, a)} \right) \qquad (3)$$

It is advantageous to define the relative dimensionless linear velocity as $U_a(Y,Z) = u_a(Y,Z)/u_a(0,0)$.

By combining Eqs.(2) and (3) it holds:

$$U_a(Y,Z) = \left(1 - Y^2\right)\left(1 - \frac{\cosh(\sqrt{3}\ a\ Z\ ) - 1}{\cosh(\sqrt{3}\ a\ ) - 1}\right) \tag{4}$$

Eq.(4) describes the dimensionless flow velocity profile in rectangular cross-section channel relative to the linear velocity at the coordinates Y = 0, Z = 0.

The equation describing the flow velocity profile in modulated permeability cross-section channel can be derived in a similar way by applying Eq.(1). The trapezoidal cross-section channel, that seems to be the most practical from the experimental point of view, will be considered as an example. Providing the angle between two inclined walls of the trapezoidal cross-section channel is not too high and, on the other hand, the aspect ratio a is high enough, Eq.(1) can be modified to give:

$$u_a'(y,z) = \frac{k'\ w^2(z)\ \Delta P}{\mu\ L}\left(1 - \frac{y^2}{b^2}\right)\left(1 - \frac{\cosh[\sqrt{3}\ a(z)\ \frac{z}{c}\ ]}{\cosh[\sqrt{3}\ a(z)]}\right) \tag{5}$$

where k' is another numerical constant valid for trapezoidal cross-section channel, w(z) is the thickness of the channel and a(z) is the aspect ratio, both varying with z coordinate. By applying the identical normalization routine as above, the relationship for dimensionless flow velocity profile is obtained:

$$U_a'(Y,Z) = W^2(Z)\left(1 - Y^2\right)\left(1 - \frac{\cosh[\sqrt{3}\ a(Z)\ Z] - 1}{\cosh[\sqrt{3}\ a(Z)] - 1}\right) \tag{6}$$

where $U_a'(Y,Z) = u_a'(Y,Z)/u_a'(0,0)$, $W(Z) = w(Z)/w(0)$, and $w(0) = (w_1+w_2)/2$, w_1 and w_2 being the thicknesses of the channel at the bottom and the upper channel walls at $Z = \pm 1$ (see Fig.1).

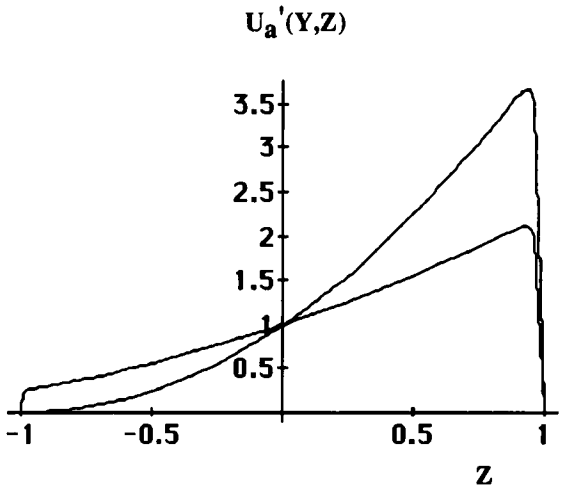

Fig.2. Flow velocity profiles in trapezoidal (lower curve) and closed triangular (upper curve) cross-section channels.

The flow velocity profiles formed in trapezoidal and closed triangular cross-section channels were calculated by using Eq.(6) and are demonstrated in Fig.2. The geometrical parameters necessary for the calculations were given in previous paper[1].

The flow velocity profiles in both of the mentioned modulated cross-sectional permeability channels were calculated for Y=0. As can be seen on Fig.2, the central part of the flow velocity profile is approximately a quadratic function for *trapezoidal cross-section channel* and exhibits a maximum near the upper (wider) wall. This fact cannot be neglected for the real closed channels. The flow velocity profile in a closed *triangular cross-section channel* displays a similar shape with a maximum near the upper wall as in a trapezoidal cross-section channel, followed by steep drop to zero velocity value at the upper wall.

The flow velocity profiles formed in two rectangular cross-section channels differing by aspect ratios were calculated by using Eq.(4), and are demonstrated for comparison in Fig.3.

Cornish [3] published an exact equation describing the flow velocity profile in rectangular cross-section channel. In the present coordinate system it can be written as:

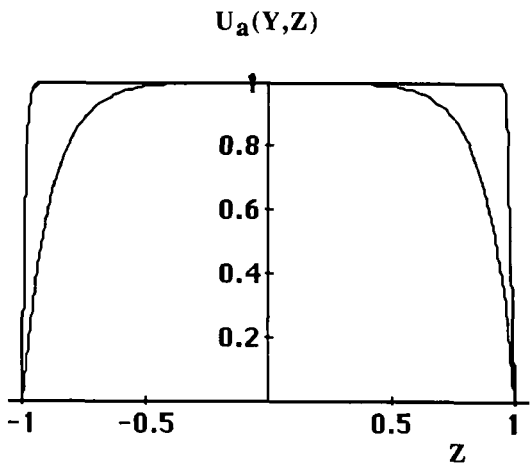

Fig.3. Dimensionless flow velocity profiles formed in rectangular cross-section channels with aspect ratios a = 5 (lower curve) and a = 50 (upper curve).

$$u_e(Y,Z) = u_{max} \left\{ 1 - Y^2 - \frac{32}{\pi^3} \sum_{n=0}^{\infty} \frac{(-1)^n}{(2n+1)^3} \frac{\cosh[(2n+1)\,\pi\,a\,Z/2]\cos[(2n+1)\,\pi\,Y/2]}{\cosh[(2n+1)\,\pi\,a/2]} \right\} \tag{7}$$

and converted to the dimensionless form similarly as Eq.(4):

$$U_e(Y,Z) = \left\{ 1 - Y^2 - \frac{32}{\pi^3} \sum_{n=0}^{\infty} \frac{(-1)^n}{(2n+1)^3} \frac{\cosh[(2n+1)\pi a Z/2]\cos[(2n+1)\pi Y/2]}{\cosh[(2n+1)\pi a/2]} \right\} / \left\{ 1 - \frac{32}{\pi^3} \sum_{n=0}^{\infty} \frac{(-1)^n}{(2n+1)^3} \frac{1}{\cosh[(2n+1)\pi a/2]} \right\} \tag{8}$$

The accuracy of the approximate solution can be demonstrated by the relative difference between the shape of the flow velocity profiles calculated for rectangular cross-section channel from the approximate Eq.(4) and from the exact

Eq.(8). The flow velocity profile established in the planes parallel to the plane of x and y axes resulting from both Eqs.(4) and (8) is parabolic. The same holds true for modulated cross-sectional permeability channels such as, e.g., a trapezoidal cross-section channel. The shape of the flow velocity profile in the planes parallel to the plane of x,z axes vary with the aspect ratio a for both rectangular and trapezoidal cross-section channels. The relative difference was defined as: $[U_e(0,Z) - U_a(0,Z)]/U_e(0,Z)$ x100 and calculated as a function of the coordinate Z for three different aspect ratios: a = 5, a = 10, and a = 100 . Since the flow velocity profiles in question are symmetrical with respect to Z = 0, the relative differences were calculated only for Z between 0 and 1. The results of the calculation for reference flow velocity profile lying in the plane of x,z axes (Y = 0) are shown in Fig. 4.

The relative difference between the approximate and exact flow velocity profiles calculated as a function of Z and shown on Fig.4 is negligible in the central (almost linear) part. The differences become important near the shorter walls. Providing the aspect ratio a is high enough (a=100 is a typical value for the actual

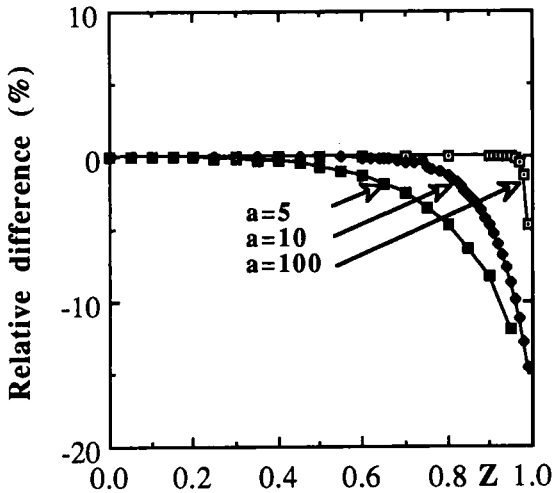

Fig.4. Relative difference between the shape of the flow velocity profile formed in rectangular cross-section channels with different aspect ratios a, calculated from the approximate Eq.(4) and exact Eq.(8) for Y = 0.

FFF channels), the difference higher than 5% appears only at the close proximity of the side channel walls (at Y>0.99). The channel with the aspect ratio value of a=10 can be considered as a limit case for which the difference of about 10% for Z=0.96 can still be neglected. The differences should not be neglected for lower values of aspect ratio a. The series in Eq.(8) converges very rapidly and n=2 was found to be high enough to calculate the sums with satisfactory precision. However, n=10 was used throughout all calculations. The relative difference between the exact and approximate flow velocity profiles demonstrated on Fig.4 was calculated only as a function of Z for a constant value of Y=0. The dependence of the relative difference on both Y and Z variables was calculated subsequently and the results are demonstrated on Fig.5.

As can be seen in Fig.5, the conclusions concerning the relative differences between the flow velocity profiles calculated from the approximate and exact equations for one value of Y=0 hold for the whole region of the values of Y

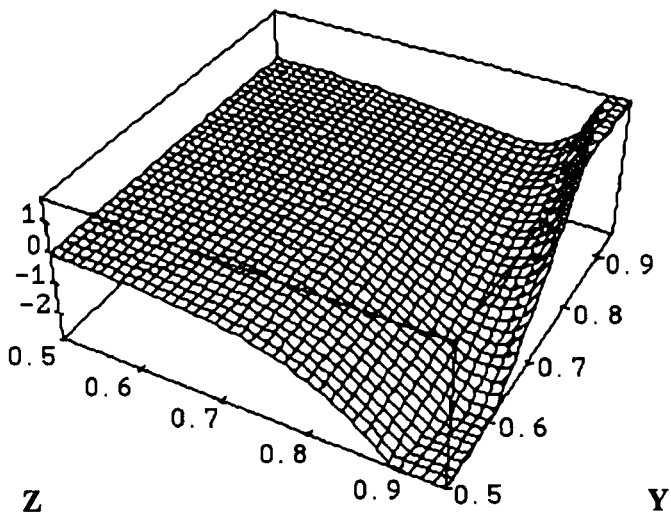

Fig.5. Three-dimensional representation of relative differences between the flow velocity profiles calculated from the approximate and exact relationships for rectangular cross-section channel (aspect ratio a=10).

and Z from -1 to 1. As the differences are negligible for the central part of the spatial flow velocity profile and the profiles formed in rectangular cross-section channels are symmetrical with respect to the x-axis, only a border region within $0.5<Y<0.95$ and $0.5<Z<0.95$ is demonstrated in the three-dimensional plot on Fig.5. The value of the aspect ratio a=10 was chosen in order to demonstrate the differences in a channel that can be considered as a limit case, as mentioned above.

As concerns the comparison of the approximate description of the flow velocity profile formed in the trapezoidal or closed triangular cross-section channels, both of them denominated as modulated cross-sectional permeability channels described by Eq.(6) derived previously [1], with the flow velocity profile formed in a hypothetical infinite inclined walls channel [4], that approximates the flow velocity profile established in a real triangular cross-section channel, the differences are obvious. The infinite inclined walls channel does not represent the real model for flow velocity profile established in trapezoidal cross-section channel but can approximate the flow velocity profile formed in triangular cross-section channel with the exception of the region near the upper wall.

From the presented analysis of the isoviscous flow velocity profiles formed in modulated cross-sectional permeability channels the following most important conclusions can be drawn. The approximate solution proposed previously and based on Takahashi and Gill's equation describes the flow velocity profile with a fair precision as compared to the exact solution. The advantage of the approximate solution is a simple form and tractability of the resulting equation. As concerns the exact solution, it has been shown, that the calculation of the series can be performed to a surprisingly low degree with a satisfactory result. Both of these conclusions can be important for the calculations of the flow velocity profiles formed under more complicated non-isoviscous flow conditions as well as for practical evaluation of focusing FFF experimental results.

The three-dimensional models of the flow velocity profiles established in rectangular and trapezoidal cross-section channels under the conditions of isoviscous flow were generated by using Eqs.(4) and (6) and are demonstrated in Fig.6.

Resolution

The equation describing the resolution R_S, derived previously, was aimed merely to estimate the function of the shape and dimensions of the trapezoidal

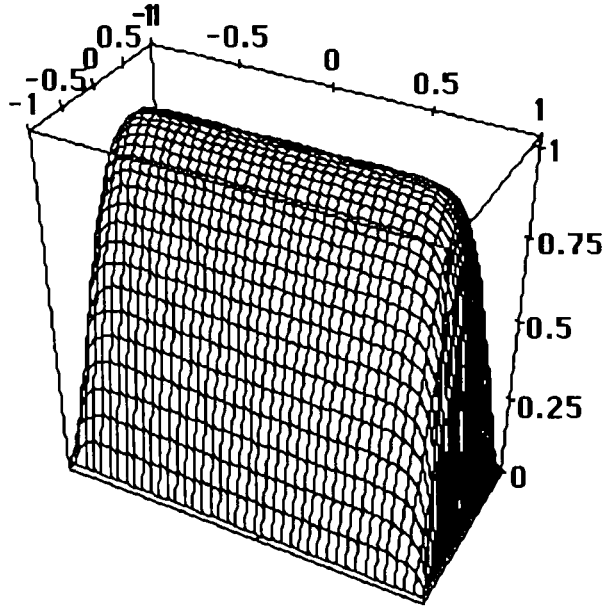

(a)

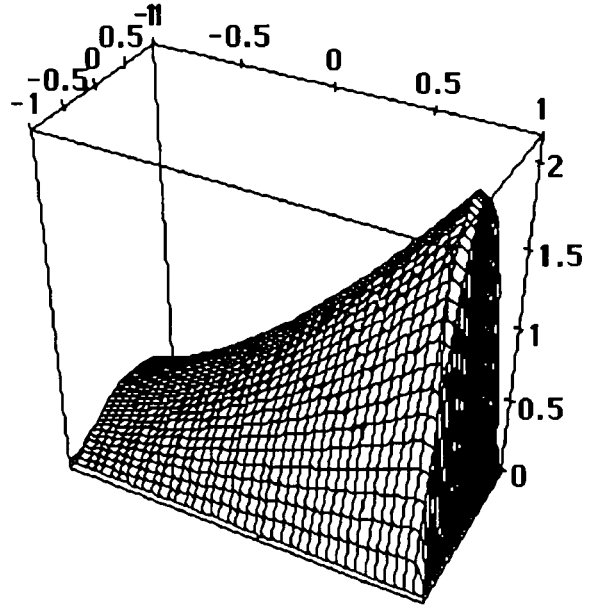

(b)

Fig.6. Three-dimensional flow velocity profiles formed in rectangular (a) and trapezoidal (b) cross-section channels.

cross-section channel [1]. With respect to the simplifying conditions adopted, its accurate application was limited to the evaluation of the influence of geometrical parameters of the channel. Its use to calculate the actual time based resolution of the fractionated species is acceptable exclusively with some precaution. The problem reposes on the neglect of the broadening of the focused zones in the direction of the focusing field action. Consequently, the calculated R_s values represent only an approximation of the actual time based resolution. The same holds true for the time based resolution calculated in ref.4 by using basically identical relationship, an aposteriori introduction of the zone width value corresponding to the broadening in the direction of the focusing into the numerical calculation does not change the limited validity of the relationship for R_s.

For a separation at minimal value of the height equivalent to the theoretical plate (HETP) and, consequently, for an extremely low flow rate due to a very low diffusion coefficients of macromolecules or particles under consideration, a very long separation time was calculated [4]. In this context, it might be interesting to calculate the time of the separation at the velocity corresponding to the minimal HETP value by gel permeation chromatography (GPC) or hydrodynamic chromatography (HC) methods of a macromolecular or particulate species with the diffusion coefficient of the order of 10^{-7} cm^2sec^{-1}. By using the optimal Péclet number $Pe_{opt} = 3.15$ found recently by Magnico and Martin [5] for the dispersion in the interstitial space of the packed chromatographic column (a model that can simulate the zone broadening in both GPC and HC columns), and by considering a 30 cm long column packed with the particles of 100 μm in diameter (in order to have the experimental conditions comparable with those evaluated in ref.4), it holds for the time of the separation:

$$t = \frac{L_c\, d_p}{Pe_{opt}\, D} = \frac{30 \times 100 \times 10^{-4}}{3.15 \times 10^{-7}} \doteq 10^6 \text{ sec} \qquad (9)$$

where d_p is the particle diameter, L_c is the length of the column, and D is the diffusion coefficient.

As a result, it is unrealistic at least under the considered conditions to separate the macromolecular or particulate species at very low flow rates corresponding to minimal HETP value, no matter which separation method is used.

The decrease of d_p to 10 μm value corresponding to the high resolution column packing does not result in acceptable separation time. There are other effective means that should be applied to obtain the accurate analytical information even when operating far from the minimal HETP value, e.g. by using a powerful band broadening correction methods, by measuring at different flow rates and extrapolating to zero flow rate, etc.

The resolution for other than minimal HETP values, i.e. for different linear flow velocities can be calculated from Eq.(10), obtained by substitution from Eq.(13) ref.[1] for HETP into definition relationship for resolution, Eq.(17) ref.[1]. By neglecting the longitudinal diffusion it holds:

$$R_S = \frac{\sqrt{105\ L\ D}\ (\ w^2(p) - w^2(q)\ )}{4\ w^2(p)\ w(q)\ \sqrt{u(q)}} = \frac{\sqrt{105\ L\ D}\ (\ w^2(p) - w^2(q)\ )}{4\ w^2(q)\ w(p)\ \sqrt{u(p)}} \qquad (10)$$

where L is the length of the channel, w(p), w(q) are the thicknesses of the channel at the positions p and q of the focused zones, D is the diffusion coefficient, and u(p,q) is the average linear velocity of the focused zone at the position p or q.

Regardless the limited validity of the R_S relationship for the calculation of resolution in actual experiments when neglecting the zone broadening in the direction of focusing, another interesting approach can be to compare the experimentally achieved resolutions with the R_S values calculated for the corresponding established experimental conditions. The experimental results from refs. [6,7] can be used as reference data.

The separation by SFFFFF of the submicron latex particles of polystyrene (particle diameter of 624 nm) and polyglycidylmethacrylate (particle diameter of 675 nm) differing in densities was demonstrated in the first paper [6]. The gravitational forces and the density gradient formed inside the trapezoidal cross-section channel were applied to achieve the focusing effect. In the other paper [7], the separation by isoelectric focusing field-flow fractionation (IEFFFF) of two components (acidic and basic) of the horse heart myoglobin (molecular weight of 18 500) was demonstrated. In this case, the focusing was initiated by the electric field and pH gradient formed inside the trapezoidal cross-section channel. The resolutions evaluated from the published fractograms [6,7] are by coincidence almost

identical, R_{exp}=0.58. The known channel dimensions allow to calculate the hypothetical R_s values. The resolution and the separation time corresponding to minimal HETP value can be evaluated without problem for IEFFFF[7], because the lateral positions (in the direction of the field action across the channel) of the focused zones can be calculated from the known retention volumes, channel dimensions, and flow rate of the carrier liquid. In the paper on SFFFFF [6], only the range of the flow rates applied and the fractogram without absolute values of the retention volumes were given. With respect to the densities of the separated latex particles it was estimated that the zones were focused in the lower part of the channel, however, R_s as well as the separation time were calculated for both extremes, the lowest and the highest zone positions corresponding to relative retentions evaluated from the published fractogram [6]. The results are summarized in Table 1. The data necessary for the calculation can be found in the previous papers [6,7].

The results in Table 1 show that if the resolution R_s is calculated from the available data for the actual experimental flow rates by using Eq.(10), the value of R_s=0.64 obtained for SFFFFF is by about 10% higher than the actual experimental resolution, and the value of R_s=0.48 obtained for IEFFFF is by about 17 % lower than the experimental value (see Table 1.).

The gravitation is certainly not the most powerful field to be used for focusing field-flow fractionation. Both discussed experiments represented only a special cases intended to demonstrate that the theoretically predicted separation principle can experimentally be implemented. No optimization was taken into account.

Table 1. Comparison of calculated hypothetical and experimental resolutions.

	Experimental resolution	Estimated diffusion coefficient ($cm^2\ sec^{-1}$)	t_{exp} (hours)	R_s **
SFFFFF ref. [6]	0.58	6.6×10^{-9}	10.1*	0.25-0.64***
IEFFFF ref. [7]	0.58	1×10^{-6}	0.50	0.48

* Calculated for the flow rate of 0.010 ml min^{-1}
** Calculated for the actual experimental flow rates
*** Calculated for the lowest and highest positions of the focused zones

Acknowledgement: Author is indebted to Ministère de la Recherche et de la Technologie, France, for supporting his stay at E.S.P.C.I., Paris and to Dr. Michel Martin for stimulating discussions.

REFERENCES

1. J. Janca and V. Jahnova, J. Liq. Chromatogr., 6, 1559 (1983).
2. T. Takahashi and W. N. Gill, Chem. Eng. Commun., 5, 367 (1980).
3. R. J. Cornish, Proc.Roy.Soc., London A, 120, 691 (1928).
4. S. Wicar, J. Chromatogr., 454, 335 (1988).
5. P. Magnico and M. Martin, J.Chromatogr., 517, 31 (1990).
6. J. Chmelik and J. Janca, J. Liq. Chromatogr., 9, 55 (1986).
7. J. Chmelik, M. Deml, and J. Janca, Anal.Chem., 61, 912 (1989).